Available online at www.sciencedirect.com

ScienceDirect

Ceramics International 40 (2014) 3595–3601

CERAMICS INTERNATIONAL

www.elsevier.com/locate/ceramint

Sintering behavior and microwave dielectric properties of $(1-x)Li_2TiO_3+xLiF$ ceramics prepared by enhanced sintering

Bian Jianjiang*, Ding Yaomin

Department of Inorganic Materials, Shanghai University, 149 Yanchang Road, Shanghai 200072, China

Received 1 August 2013; received in revised form 4 September 2013; accepted 14 September 2013
Available online 19 September 2013

Abstract

Sintering behavior, structure and microwave dielectric properties of $(1-x)Li_2TiO_3+xLiF$ ($0 \le x \le 0.7$) ceramics prepared by enhanced sintering were studied by thermal dilatometry, X-ray diffraction (XRD), Scanning Electron Microscopy (SEM), Raman spectra and microwave resonant measurement. It was found that the short range ordering and order–disorder phase transition temperature in this case increased compared with that observed for the specimen prepared from prealloyed powders because of the compositional inhomogeneity. The early stage sintering was enhanced by the chemical potential gradient originated from the compositional gradient between Li_2TiO_3 and LiF. However unequal diffusion rates between LiF and Li_2TiO_3 particles left behind large pores in the sintered bodies. Transient liquid phase sintering was confirmed in the $x \ge 0.2$ compositions. An optimized microwave dielectric properties with ε_r of ~22.4, $Q \times f$ of ~110,000 GHz and τ_f of ~3.2 ppm/°C could be obtained for the $x=0.1$ composition after sintering at 1100 °C/2 h.

Keywords: A. Sintering; Ceramic; Microwave dielectric properties

1. Introduction

Li_2TiO_3 in which Li layers alternated with ordered (Li, Ti) layers has the dielectric constant of 22, $Q \times f$ value of 63,500 GHz (8.6 GHz), and τ_f value of 20.3 ppm/°C after sintering at 1300 °C/2 h [1]. However high porosity remains in the pure or doped Li_2TiO_3 ceramic in the previous studies [2–3], which is detrimental to practical applications. The sinterabiltiy of Li_2TiO_3 could be improved by adding CuO–B_2O_3 [4]. Li_2TiO_3 could also be successfully densified by doping with LiF probably due to the decrease in bond strength [5]. Li_2TiO_3 can form wide range of solid solution with LiF ($(1-x)Li_2TiO_3+xLiF$). The sintering temperature decreased from about 1300 °C/2 h for the undoped Li_2TiO_3 to about 1100 °C/2 h when $x=0.1$ and further reduced to 950 °C/2 h when $x=0.4$. Optimized microwave dielectric properties with $\varepsilon_r = \sim 23.6$, $Q \times f = \sim 108{,}000$ GHz and $\tau_f = \sim 4.2$ ppm/°C; and $\varepsilon_r = \sim 20.3$, $Q \times f = \sim 67{,}000$ GHz and $\tau_f = -39.0$ ppm/°C could be obtained after sintering at 1100 °C/2 h for the $x=0.1$ composition and 950 °C/2 h for the $x=0.4$ composition, respectively [5].

Homogenization during sintering is an alternative to forming compacts from precompounded or prealloyed powders [6]. Unlike sintering composites where there is essentially no chemical interaction, homogenization coupled with sintering occurs by diffusion of each species into other. Classic examples of sintering homogenization to form solid solutions are Cr_2O_3–Al_2O_3 and NiO–MgO, which are isomorphic mixtures where sintering occurs simultaneously with interdiffusion. Compositional gradients enhance the overall mass diffusional fluxes, and the interface between phases aids vacancy creation while retarding grain growth [6]. Although Li_2TiO_3 (C2/c) exhibit different space group from LiF (Fm-3m), extensive range of substitutional solid solution could still be formed between the two end members due to their same rock salt type structure in which oxygen octahedron are edge shared.

In this paper we, therefore, studied the structural evolution, sintering behavior, microstructure and microwave dielectric

*Corresponding author. Tel./fax: +86 21 56331697.
E-mail address: JJBian@shu.edu.cn (B. Jianjiang).

0272-8842/$ - see front matter © 2013 Elsevier Ltd and Techna Group S.r.l. All rights reserved.
http://dx.doi.org/10.1016/j.ceramint.2013.09.066

properties of $(1-x)Li_2TiO_3+xLiF$ $(0 \le x \le 0.7)$ ceramics prepared by sintering homogenization method, in contrast to our previous ones prepared from prealloyed powders [5].

2. Experimental procedure

$(1-x)Li_2TiO_3+xLiF$ $(0 \le x \le 0.7)$ ceramics were prepared by conventional solid-state reaction process from the starting materials including Li_2CO_3 (99.9%), TiO_2 (99.7%) and LiF (99.9%). Two-steps process was adopted in this case. First Li_2TiO_3 was synthesized at 800 °C/2 h. Then the synthesized Li_2TiO_3 was added with different amounts of LiF according to the above formula, and then mixed with ZrO_2 balls in ethanol for 24 h. The ground powders were dried, then mixed with 7–10 wt% PVA as binder and granulated. The granulated powders were uni-axially pressed into compacts with 10 mm in diameter and 4.5–5.5 mm in height under the pressure of 100 Mpa. The compacts were sintered at the temperatures range from 850 °C to 1200 °C for 2 h. The sintering temperature was optimized by the maximum bulk density and $Q \times f$ value. In order to prevent lithium evaporation during the sintering, the compacts were covered with sacrificial powder of the same composition.

The phase compositions of the sintered specimens were identified by X-ray powder diffraction with Ni-filtered Cu Ka radiation (Rigaku D/max2550, Tokyo, Japan). The lattice parameters and theoretical density of the sample were calculated via Jade 6.5 software. The Raman experiments were carried out for the sintered samples (RENIShaw in Via plus, UK). The excited laser line is 785 nm of semiconductor laser at a power of 250 mW and the scattered light was recorded in back-scattering geometry using an InVia Raman Microscope equipped with a grating filter, enabling good stray light rejection in the 100–1000 cm range. The sintering behavior was measured by dilatometry at a heating rate of 5 °C/min using a horizontal-loading dilatometer with alumina rams and boats (NETZSCH STA 449C, Netzsch Instrument, Germany). The densities of the ceramics were measured by the Archimedes method. The microstructure of the sintered samples was observed by scanning electron microscopy (Model JSM-6700F, JEOL, Tokyo, Japan). All the samples were polished and thermally etched at the temperature of 100 °C lower than its sintering temperature for 30 min. Microwave dielectric properties of the sintered specimens were measured at about 8–11 GHz using a network analyzer (model N5230A, Agilent, Palo Alto, CA). The quality factor was measured by the transmission cavity method. The relative dielectric constant was measured according to Hakki–Coleman method with the TE_{011} resonant mode, and the temperature coefficient of the resonator frequency were measured using invar cavity at the temperature range from 20 °C to 80 °C.

3. Results and discussion

Fig. 1 shows the powder XRD patterns of $(1-x)Li_2TiO_3+xLiF$ $(0.05 \le x \le 0.70)$ ceramics prepared by sintering homogenization process and sintered at different temperatures. It shows that limited range of solid solutions formed between Li_2TiO_3 and LiF. For small x value $(x \le 0.1)$, the solid solutions sintered at 1050 °C/2 h have the same layer ordered monoclinic rock salt structure as that of pure Li_2TiO_3 (β-Li_2TiO_3(ss), S.G.: C2/c). But it transformed to disordered cubic phase (α-Li_2TiO_3 (ss)) when $x=0.15$–0.2 after sintering at 1050 °C/2 h. All these observations are similar to those observed for the specimens prepared from prealloyed powders [5]. In this case, however trace amount of LiF second phase appeared when $x \ge 0.4$, in contrast to $x=0.5$ for that prepared from prealloyed powders. It seems to show that the miscibility between LiF and Li_2TiO_3 in this case $(x < 0.4)$ is slightly lower than that prepared from prealloyed powders after sintering at the same temperature. Note that the $x=0.3$ and $x=0.4$ compositions in this case exhibited the presence of ordered monoclinic phase in contrast to a completely disordered cubic phase observed for the corresponding compositions prepared from prealloyed powders after sintering at same temperature (875 °C). It is obviously due to the compositional inhomogeneity of the ceramics prepared by sintering homogenization process. Homogenization occurs with sintering process simultaneously in this case. It is the interdiffusion rate that determines the homogenization. With increase in sintering temperature and/or prolonged sintering, the compositional gradients should level out, eventually reaching a constant value at the composition given by the two phase mole ratio in the original powder mixture. The ordering degree decreased with the increase in miscibility and compositional homogeneity, which is evidenced by the fact that the intensity of the (002) superstructure peak considerably decreased for $x=0.4$ and even became almost zero for $x=0.3$ as the sintering temperature increased from 875 to 900 °C/2 h. It seems to indicate that the order–disorder phase transition temperature in this case slightly increased compared with that observed for the specimen prepared from prealloyed powders because of the compositional inhomogeneity [5].

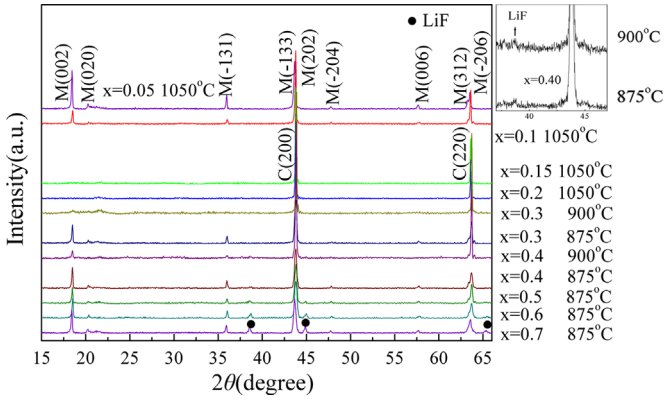

Fig. 1. Powder XRD patterns of $(1-x)Li_2TiO_3+xLiF$ $(0.05 \le x \le 0.70)$ ceramics.

Raman spectroscopy is more suitable than XRD to detect the local structure. Fig. 2 demonstrates the Raman spectra of $(1-x)Li_2TiO_3+xLiF$ solid solutions prepared by sintering homogenization process. For comparison, the Raman spectra of the same compositions prepared from the prealloyed

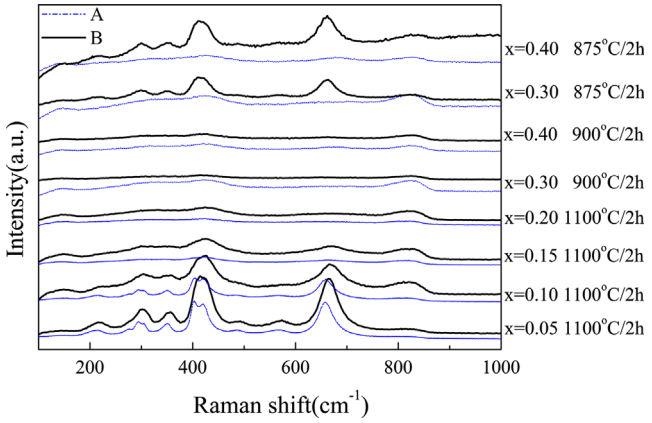

Fig. 2. Raman spectrum of $(1-x)Li_2TiO_3+xLiF$ ($0.05 \le x \le 0.40$) ceramics (A) prepared by sintering homogenization and (B) prepared from prealloyed powders.

powders are also presented [5]. The spectra of $x=0.05$ and $x=0.1$ are very similar to that of pure monoclinic Li_2TiO_3 [7]. The presence of weak broad bands near 660 cm^{-1} and 420 cm^{-1} excluded the completely random distribution of ions for the $0.15 \le x \le 0.2$ compositions which exhibit disordered cubic phase (Fm-3m) as shown in Fig. 1. It indicates that short range ordering (SRO) should exist in cubic phase solid solutions, although long range ordering (LRO) was destroyed, which is similar to the observation for those prepared from prealloyed powders [5]. The broadening of the Raman band for solid solution can be caused by the scattering from compositional fluctuations, grain size reduction and the anharmonic decay of the optical phonons [8–10]. The decrease in intensity and broadening of the Raman band with the increase of LiF content reveal that the ordering degree decreased with the increase of LiF content, which is in well agreement with that observed by XRD. A comparison of Raman spectra of the same composition prepared by two different methods seems to infer that the compositional inhomogeneity, ordering degree and its domain size of the specimen prepared by sintering homogenization process seems to be larger than that of specimen prepared by prealloyed method, especially for the $x=0.3$ and $x=0.4$ sintered at 875 °C/2 h. The difference in SRO leveled out with increasing sintering temperature, which is in well agreement with that observed by XRD.

Fig. 3 shows the shrinkage behaviors of the compacts with $x=0.10$, 0.20, 0.30. For comparison, the shrinkage curves of the same compositions prepared from the prealloyed powders are also appended [5]. All samples exhibited a rapid shrinkage above 800 °C. The shrinkage rates in this case are much larger than those of corresponding specimens prepared from prealloyed powders. For $x=0.1$ composition, the maximum shrinkage rate occurred at about 815 °C, which is slightly lower than that of the corresponding specimen prepared from prealloyed powders (850 °C), and also lower than the melting point of LiF (845 °C). The possible liquid phase sintering from the melting of LiF at 845 °C can be excluded in this composition. Although binary phases of Li_2TiO_3 and LiF

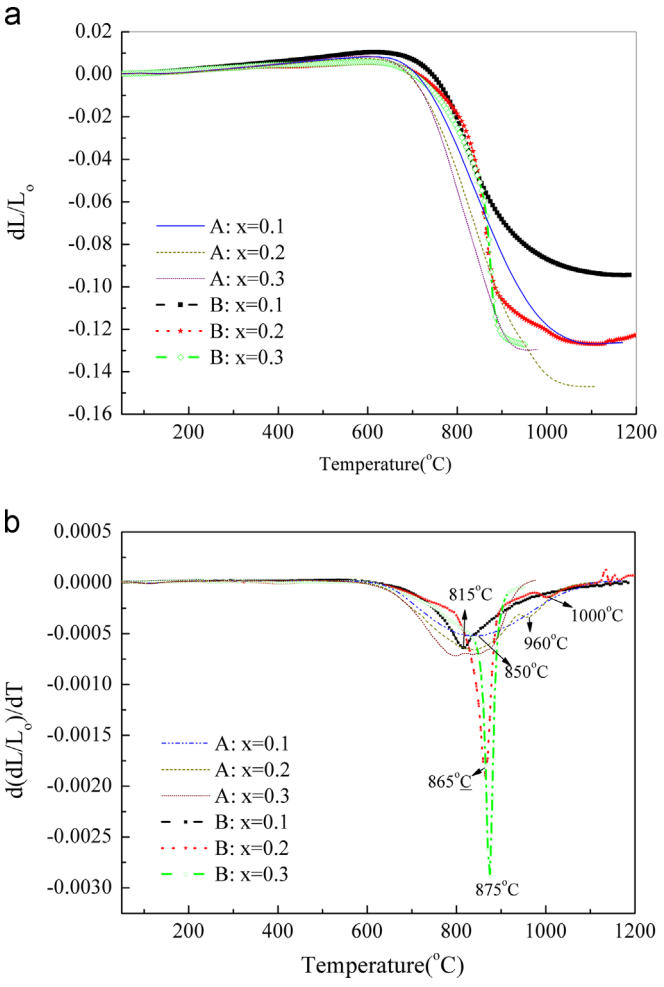

Fig. 3. (a) Shrinkages and (b) shrinkage rates of $(1-x)Li_2TiO_3+xLiF$ ($x=0$, 0.10, 0.20, 0.30) compacts measured at heating rate of 5 °C/min (curves A) (For comparison, the shrinkage curves of the same compositions prepared from the prealloyed powders also illustrated [1] (curves B)).

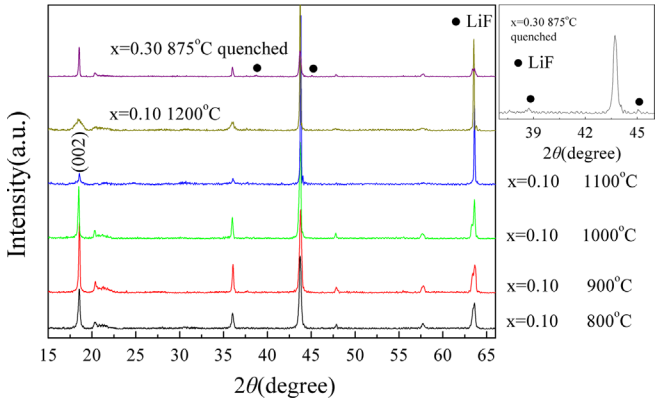

Fig. 4. Powder XRD patterns of the $x=0.1$ composition sintered at different temperatures and $x=0.3$ qunched from 875 °C.

existed in the original powder mixture of $x=0.1$ composition, LiF would substitute into the Li_2TiO_3 structure and formed monoclinic solid solution at about 800 °C for 2 h by sintering homogenization process (Fig. 4). The existing chemical

potential gradient originated from the compositional gradient between Li_2TiO_3 and LiF enhanced the mass transfer during sintering in addition to a decrease in the bond strength with the addition of LiF as expected. Thus the $x=0.1$ composition in this case exhibited larger maximum shrinkage rate and slight lower temperature at which maximum shrinkage rate occurred compared with that prepared from the prealloyed powders. The maximum shrinkage rate increased remarkably from 0.065%/°C to 0.29%/°C and its occurring temperature slightly increased from 815 °C to about 875 °C as the LiF content increased from $x=0.1$ to $x=0.3$. The maximum shrinkage rates for $x=0.2$ and $x=0.3$ in this case are also much larger than those of the corresponding compositions prepared from the prealloyed powders. Note that the temperatures at which maximum shrinkage rate occurred for $x=0.2$ (865 °C) and $x=0.3$ (875 °C) in this case are slightly above the melting point of LiF (845 °C). In order to clarify the sintering mechanisms of the above compositions, the $x=0.3$ specimen was quenched after firing at 875 °C and then examined by XRD (Fig. 4). It shows that small amount of LiF phase could be observed in addition to Li_2TiO_3 phase in the quenched specimen, which indicates the presence of LiF liquid phase during the sintering process. However the LiF liquid phase is transient and would form substitutional solid solution with Li_2TiO_3 after sintering at 875 °C for 2 h as shown in Fig. 1. The larger maximum shrinkage rate of $x=0.3$ composition compared with that of $x=0.2$ can be ascribed to the increase in LiF liquid phase amount. Note also that the second maximum shrinkage rate caused by order–disorder phase transition for the $x=0.2$, which occurred at about 1000 °C in this case, is smaller in comparison with that of the corresponding composition from prealloyed powders, which occurred at about 960 °C. Sintering shrinkage rates are higher near the order–disorder temperature for a compound and increase with disordering. Thus the decrease in the second maximum shrinkage rate and increase in its occurring temperature can be attributed to the less disordering and increase in temperature of order–disorder phase transition caused by compositional inhomogeneity in this case compared with that from prealloyed powders as discussed above. As we know that the order–disorder phase transition temperature decreased with increasing LiF content. Thus for the $x=0.3$ composition in this case, the second maximum shrinkage rate originated from order–disorder phase transition is not obvious, and may coincide with the first maximum shrinkage rate caused by liquid phase at about 875 °C. No second maximum shrinkage rate was observed for the $x=0.1$ composition due to its higher temperature of order–disorder phase transition as shown in XRD analysis (Fig. 4).

Variations of relative bulk densities of $(1-x)Li_2TiO_3+xLiF$ ceramics ($0.05 \le x \le 0.4$) sintered at different temperatures as a function of LiF content are shown in Fig. 5. The optimized sintering temperature strongly depended on the composition. It slightly increased from about 1100 °C to 1150 °C as LiF content increased from $x=0.05$ to 0.15. Further increase in x reduced the sintering temperature to 950 °C for $x=0.2$ and 900 °C for $x=0.3$–0.4 compositions, respectively. Note that the specimens in this case densified much faster (Fig. 3) and

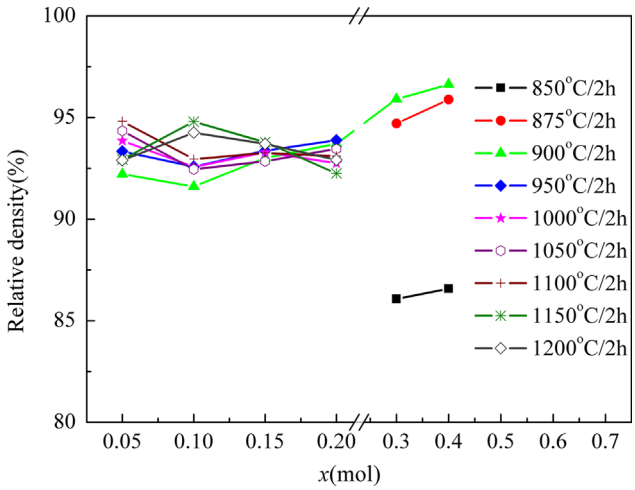

Fig. 5. Variations of the relative bulk densities of $(1-x)Li_2TiO_3+xLiF$ ($0.05 \le x \le 0.40$) ceramics as a function of LiF content for samples sintered at different temperatures.

consequently obtained higher density at low sintering (900 °C/2 h) compared with those prepared from the prealloyed powders. The faster sintering rates and higher densities for $x=0.05$–0.15 compositions after sintering at 900 °C/2 h in this case can be ascribed to the occurrence of activated sintering by the intersolubility between Li_2TiO_3 and LiF, and those for $x=0.2$–0.4 can be mainly attributed to the presence of transient liquid phase sintering, respectively as discussed above. However the enhanced densification rate caused by activated sintering for the $x=0.05$–0.15 compositions in this case decreased with increasing sintering temperature. This can be explained by a decrease in chemical potential gradients by homogenization with increasing sintering temperature. It means that the activated sintering by homogenization dominated the early stage of sintering.

Fig. 6(a) shows the SEM images of the $(1-x)Li_2TiO_3+x$-LiF ($0.05 \le x \le 0.5$) ceramics sintered at different temperatures. The $x=0.05$–0.15 compositions demonstrated well-developed and dense microstructure after sintering at 1150 °C/2 h. Note that the $x=0.2$ exhibited a special microstructure consisting of two type of grains after sintering at 1050 °C/2 h. Interconnections of small grains were observed above the surface of the large well-developed grains. This is related to the order–disorder phase transformation occurred at about 1000 °C for $x=0.2$ as discussed above. The larger grains due to liquid phase sintering are ordered and the interconnected grains are disordered ones. The grain growth is supposed to substantially increase when the phase changes from ordered to disordered state as reported before [11]. At the intermediate stage of phase transformation, mixture phases consisting of ordered and disordered grains caused the porous microstructure as shown in the SEM image of $x=0.2$ sintered at 1050 °C/2 h. This explained the reason why the density of $x=0.2$ sintered at 1050 °C/2 h is lower than that sintered at 950 °C/2 h as shown in Fig. 5.

The microstructural evolution with the sintering temperature for $x=0.1$ composition is shown in Fig. 6(b). The porosity

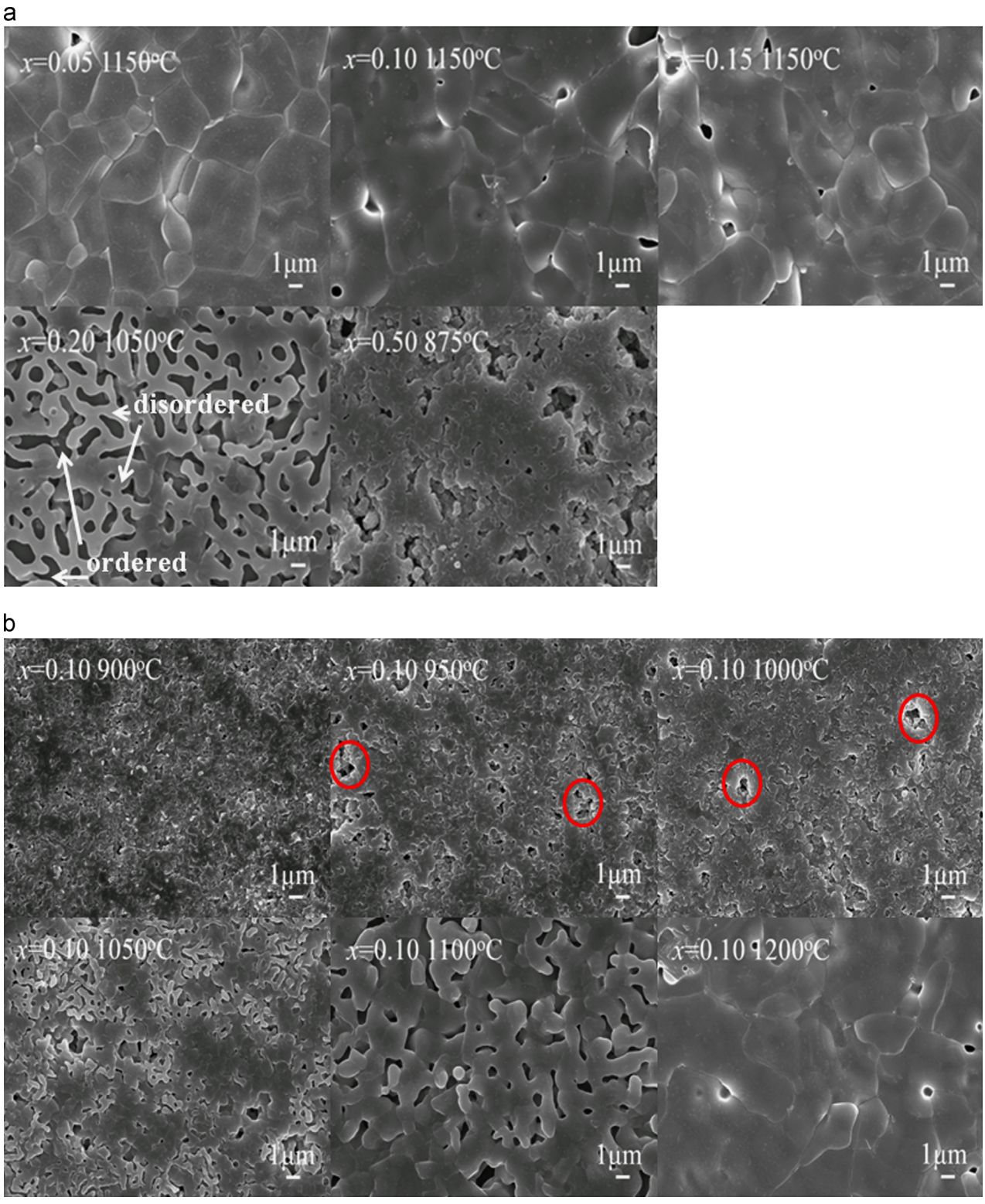

Fig. 6. (a) SEM images of $(1-x)Li_2TiO_3+xLiF$ ($0.05 \le x \le 0.50$) ceramics sintered at different temperatures and (b) evolution of the microstructure with sintering temperature for the $x=0.10$ composition.

decreased and the grain size increased as the sintering temperature increased. A dense ceramic could be obtained after sintering at 1150–1200 °C/2 h. The small grain size around 1 μm for $x=0.1$ sintered below 1050 °C/2 h seems to indicate no liquid phase sintering occurred, which is in well agreement with that observed and discussed for the shrinkage behavior (Fig. 3). Note that abrupt grain growth occurred at 1100 °C, which is corresponding to the substantial decrease in ordering degree as shown in Fig. 4. Unequal diffusion rates between LiF and Li_2TiO_3 particles manifested by their largely

different melting points left behind large pores in the sintered bodies (marked by circle in the SEM images). This explained the reason why the optimized densities obtained in this case are lower than those of prepared from prealloyed powders [5].

Fig. 7 shows the variation of dielectric permittivity as a function of LiF content and sintering temperature. The change of dielectric permittivity with sintering temperature for the fixed composition mainly corresponds to the variation of density. The optimized dielectric permittivity for each composition in this case demonstrated a similar decreasing trend with increasing LiF content to that observed for the specimens from prealloyed powders. The lower optimized dielectric permittivities for the $x < 0.2$ compostions in this case compared with those observed for the specimens from prealloyed powders can be ascribed to the lower densities as shown in Fig. 5. Fig. 8 shows the change of $Q \times f$ values of $(1-x)Li_2TiO_3+xLiF$ $(0.05 \le x \le 0.70)$ ceramics sintered at different temperatures with x. The varying $Q \times f$ value with sintering temperature for each composition can be mainly attributed to the increase in density. But the $x=0.2$ demonstrated a maximum $Q \times f$ value of about 100,000 GHz after sintering at 1050 °C/2 h rather than 950 °C/2 h at which it reached maximum density as shown in Fig. 5. This is related to the order–disorder phase transformation occurred at 1000 °C. The $x=0.2$ composition reached a maximum density after sintering at 950 °C/2 h due to the transient liquid phase sintering as described above. Its density decreased as the sintering temperature increased to 1000 °C owing to the order–disorder phase transformation occurred at this temperature as shown in Figs. 5 and 6a. Maximum $Q \times f$ value could be obtained when the ordering degree remarkably decreased, although the structure remains partially long range ordered, mainly due to the beneficial effects of LiF which stabilizes the ordered domain boundaries as we discussed in our previous paper [5]. The optimized $Q \times f$ values in this case demonstrated a similar decreasing trend with increasing LiF content to that observed for the specimens from prealloyed powders. Maximum $Q \times f$ value of about 115,000 GHz could be obtained for the $x=0.05$ composition after sintering at 1100 °C/2 h. The $x < 0.2$ compositions sintered at the temperature of 900 °C demonstrated much higher $Q \times f$ values (30,000–40,000 GHz) compared with those prepared from prealloyed powders (5000 GHz) after sintering at the same temperature due to the increase in densities by the enhanced sintering from homogenization. Although the $x < 0.2$ compositions sintered above 1050 °C/2 h in this case demonstrated lower densities (~95%) compared with those from prealloyed powders (~98%), they had almost the same $Q \times f$ values. It seems to imply that the $Q \times f$ value would increase with density when the specimen was in an ordering state ($\le$1050 °C), and be dominated by the short range ordering as the order–disorder transition occurred. Fig. 9 shows change of the τ_f value with x for the specimen sintered at the temperature optimized $Q \times f$ value reached. The τ_f value changed from positive to negative with the increase of x, and near zero value of 3.2 ppm/°C could be obtained at $x=0.1$ composition.

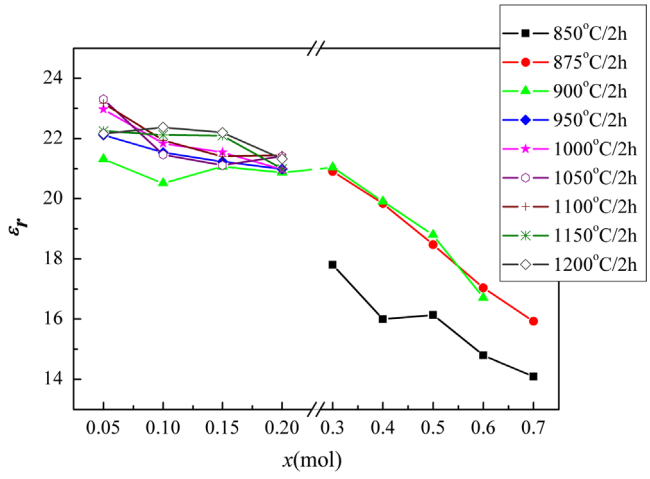

Fig. 7. Variations of the relative permittivities of $(1-x)Li_2TiO_3+xLiF$ $(0.05 \le x \le 0.70)$ ceramics with x and sintering temperature.

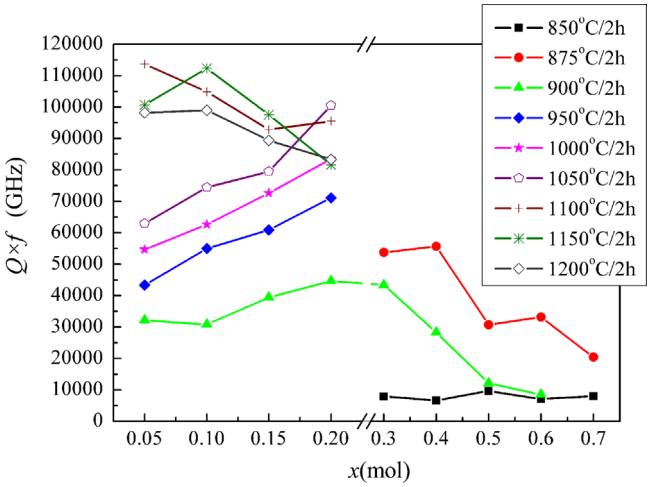

Fig. 8. Changes of $Q \times f$ values of the $(1-x)Li_2TiO_3+xLiF$ $(0.05 \le x \le 0.70)$ ceramics with x and sintering temperature.

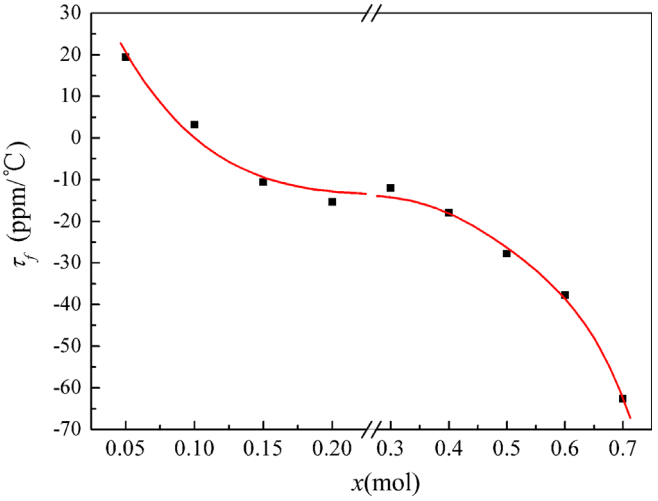

Fig. 9. Change of τ_f value with x for $(1-x)+xLiF$ $(0.05 \le x \le 0.70)$ ceramics.

4. Conclusions

Structural evolution, sintering behavior, and microwave dielectric properties $(1-x)$ of Li_2TiO_3+xLiF $(0.05 \leq x \leq 0.70)$ ceramics prepared by sintering homogenization have been studied in this work. The miscibility between Li_2TiO_3 and LiF in this case slightly decreased compared with that prepared from prealloyed powders. Trace of LiF second phase appeared when $x \geq 0.4$. The structure of the solid solution transformed from ordered monoclinic phase (β-Li_2TiO_3 (ss)) into disordered cubic rock salt (α-Li_2TiO_3 (ss)) when $x \geq 0.15$. The short range ordering and order–disorder phase transition temperature in this case increased compared with that observed for the specimen prepared from prealloyed powders because of the compositional inhomogeneity. The interdiffusion between Li_2TiO_3 and LiF originated from the compositional gradient activated the early stage sintering, which resulted in densifying much faster and consequently obtained higher density at lower sintering (900 °C/2 h) compared with those prepared from the prealloyed powders. However unequal diffusion rates between LiF and Li_2TiO_3 particles left behind large pores in the sintered bodies. Increase in sintering rate near order–disorder temperature was observed. Transient liquid phase sintering was confirmed in the $x \geq 0.2$ compositions, which remarkably increased the shrinkage rate. An optimized microwave dielectric properties with ε_r of ~22.4, $Q \times f$ of ~110,000 GHz and τ_f of ~3.2 ppm/°C could be obtained for the $x=0.1$ composition after sintering at 1,100 °C/2 h.

Acknowledgments

This work was supported by the National Science Foundation of China (NSFC), (Project number: 50872081), and partially sponsored by the Ph. D. Programs Foundation of Ministry of Education of China. The authors are thankful to Mr. Lu Bo for recording XRD patterns (Rigaku D\max 2550, Tokyo, Japan), Mr. Chu Yuliang for SEM (Model JSM-6700F, JEOL, Tokyo, Japan). Authors also would like to thanks prof. Yu Youhua from JinDeZheng Ceramic Institute for his help doing the dilatometery measurement.

References

[1] L.L. Yuan, J.J. Bian, Y.Z. Li, Y.F. Dong, Microwave dielectric properties of lithium contained ceramics with rock salt structure, Ferroelectrics 387 (2009) 1–7.

[2] J.J. Bian, Y.F. Dong, New high Q microwave dielectric ceramics with rock salt structures: $(1-x)Li_2TiO_3+xMgO$ system$(0 \leq x \leq 0.05)$, Journal of the European Ceramic Society 30 (2010) 325–330.

[3] C.L. Huang, Y.W. Tseng, J.Y. Chen, High-Q dielectrics using ZnO-modified Li_2TiO_3 ceramics for microwave applications, Journal of the European Ceramic Society 32 (2012) 3287–3295.

[4] L.X. Pang, D. Zhou, Microwave dielectric properties of low-firing Li_2MO_3 (M=Ti, Zr, Sn) ceramics with B_2O_3–CuO addition, Journal of the American Ceramic Society 93 (11) (2010) 3614–3617.

[5] Y.M. Ding J.J. Bian, Structural evolution, sintering behavior and microwave dielectric properties of $(1-x)Li_2TiO_3+xLiF$ ceramics, Presented at 7th Microwave materials and their applications conference June 3–8, 2012, TaiPei, and published on Materials Research Bulletin 48, 2013, pp. 2776–2781.

[6] R.M. German, Sintering Theory and Practice, John Wiley & Sons, Inc, New York197.

[7] J.J. Bian, Y.F. Dong, Sintering behavior, microstructure and microwave dielectric properties of $Li_{2+x}TiO_3$ $(0 \leq x \leq 0.2)$, Materials Science and Engineering B 176 (2011) 147–151.

[8] H.D. Fuchs, C.H. Grein, R.I. Devlen, J. Kuhl, M. Cardona, Anharmonic decay time, isotopic scattering time, and inhomogeneous line broadening of optical phonons in ^{70}Ge, ^{76}Ge, and natural Ge crystals, Physical Review B 44 (1991) 8633.

[9] G. Gouadec, P. Colomban, Raman Spectroscopy of nanomaterials, how spectra relate to disorder, particle size and mechanical properties, Progress in Crystal Growth and Characterization of Materials 53 (2007) 1–56.

[10] K. Ishikawa, N. Fujima, H. Komura, First-order Raman scattering in MgO microcrystals, Journal of Appied Physics 57 (1985) 973.

[11] J.J. Bian, J.Y. Wu, L. Wang, Structural evolution, sintering behavior and microwave dielectric properties of $(1-x)Li_3NbO_4$–$xLiF$ $(0 \leq x \leq 0.9)$, Journal of the European Ceramic Society 32 (2012) 1251.